# NATIONAL ADVISORY COMMITTEE FOR AERONAUTICS

**TECHNICAL NOTE 4245**

## FLUTTER ANALYSIS OF RECTANGULAR WINGS OF VERY LOW ASPECT RATIO

By Robert W. Fralich and John M. Hedgepeth

Langley Aeronautical Laboratory
Langley Field, Va.


Washington
June 1958

NATIONAL ADVISORY COMMITTEE FOR AERONAUTI

TECHNICAL NOTE 4245

# FLUTTER ANALYSIS OF RECTANGULAR WINGS OF VERY LOW ASPECT RATIO

By Robert W. Fralich and John M. Hedgepeth

## SUMMARY

A flutter analysis, employing slender-body aerodynamic theory and thin-plate theory, is made for rectangular wings of very low aspect ratio with a constant thickness. The spanwise variation of wing deflection is assumed to be given by a parabola, and the chordwise variation is allowed complete freedom. The results show the variation of flutter speed and mode shape with aspect ratio. Comparisons are made with additional results obtained by approximating the chordwise deflection shape by use of parabolic or cubic curves. The analysis shows that the cubic approximation gives good results for a ratio of chord to semispan less than 3.

## INTRODUCTION

Flutter analyses of wing and tail surfaces of very low-aspect ratio are complicated by the presence of large amounts of chordwise curvature in the flutter mode. Indeed, the question of what chord-bending degrees of freedom are necessary in order to obtain good results is largely unanswered at present.

Several studies are available that deal with the effects of chordwise variation of deformations on flutter. (For example, see refs. 1 to 7.) In these references various configurations of very low aspect ratio were analyzed. In reference 1, complete generality of chordwise deflection shape was allowed and the spanwise variation of deflection was assumed to be linear. This reference does not shed light on the chordwise shape of flutter modes, however, because no flutter condition was found. In references 2 to 7 limited account is taken of the chordwise deflections either by the superposition of several modes, by using polynomial expressions, or by the utilization of a number of discrete stations.

The present paper is concerned with an analysis of the flutter behavior of the simple rectangular cantilever plate of very low aspect ratio. (See fig. 1.) By making use of slender-body aerodynamic theory and by assuming a parabolic spanwise deflection shape, the analysis of this

configuration can be made without restricting the chordwise shape of the flutter mode. Since flutter is obtained in this case, the complexity of the chordwise deflection shape at flutter can be investigated. Results are obtained in the form of flutter boundaries, and the chordwise mode shapes for two representative cases are illustrated. In addition, the errors caused in the flutter boundaries by approximating the chordwise deflection shape by use of parabolic or cubic curves are investigated.

## SYMBOLS

| | |
|---|---|
| $C_1, C_2, C_3, C_4$ | constants of integration |
| $c$ | chord |
| $D$ | plate stiffness in bending, $Et^3/12(1 - \mu^2)$ |
| $d_0, d_1, d_2, d_3$ | constants used in equation (29) |
| $E$ | Young's modulus of elasticity |
| $F(x,\tau), F(\xi,\tau)$ | chordwise deflection shape |
| $f(\xi)$ | amplitude of chordwise deflection shape |
| $K$ | flutter-frequency parameter, $\omega\sqrt{\frac{\rho_m t s^4}{D}}$ |
| $m_1, m_2, m_3, m_4$ | roots of characteristic equation (18) |
| $P_1(x,\tau)$ | generalized distributed loading (see eq. (13a)) |
| $P(x,y,\tau)$ | distributed loading per unit area, positive in z-direction |
| $p(x,y,\tau)$ | lift per unit area, positive in z-direction |
| $q$ | dynamic pressure, $\rho\frac{U^2}{2}$ |
| $s$ | semispan |
| $t$ | thickness |

| | |
|---|---|
| $U$ | free-stream velocity |
| $V_1(\tau)$ | generalized aerodynamic leading-edge shear (see eq. (13b)) |
| $V(y,\tau)$ | leading-edge shear, positive in z-direction |
| $w(x,y,\tau)$ | deflection, positive in z-direction |
| $x,y,z$ | coordinate system (see fig. 1) |
| $\alpha,\beta,\gamma$ | parameters defined by equations (21) |
| $\epsilon$ | mass-ratio parameter, $\frac{\pi}{2}\frac{\rho s}{\rho_m t}$ |
| $\lambda$ | dynamic-pressure parameter, $\frac{5\pi}{48}\frac{qs^3}{D}$ |
| $\mu$ | Poisson's ratio |
| $\xi$ | nondimensional coordinate, $x/s$ |
| $\Pi$ | total potential energy of system |
| $\rho$ | free-stream density of fluid |
| $\rho_m$ | density of material |
| $\tau$ | time |
| $\phi(x,y,z,\tau)$ | perturbation velocity potential |
| $\omega$ | flutter frequency |
| Subscripts: | |
| I | imaginary |
| R | real |

## ANALYSIS

The flutter analysis contained herein is performed in a manner similar to that used in the analysis of static aeroelastic divergence in reference 8. The configuration treated, a constant-thickness rectangular plate of very low aspect ratio, is cantilevered from a rigid wall and is located in a fluid flow with a free-stream velocity U. (See fig. 1.)

On the basis of the low-aspect-ratio nature of the configuration, the following two assumptions are made: First, since the deflection shape would vary in a more complicated manner in the chordwise direction than in the spanwise direction, a simple spanwise variation is assumed and the chordwise variation is allowed to be arbitrary. Thus,

$$w(x,y,\tau) = y^2F(x,\tau) \tag{1}$$

The second assumption is that slender-body aerodynamic theory may be used to find the resulting aerodynamic loads when the plate deforms in the shape given by equation (1). In this theory, terms in the linearized velocity-potential equation that contain streamwise and time derivatives are neglected in comparison with terms containing crossflow derivatives. This theory is an extension of Jones' steady-aerodynamic theory (ref. 9) to unsteady aerodynamics as suggested in references 10, 11, and 2.[a] With these assumptions the flutter problem is simplified to the extent that an exact solution is possible.

### Aerodynamic Forces

In slender-body aerodynamic theory, the velocity-potential equation for linearized flow reduces to Laplace's equation in the crossflow plane:

$$\frac{\partial^2\phi}{\partial y^2} + \frac{\partial^2\phi}{\partial z^2} = 0 \tag{2}$$

---

[a]It should be noted that references 2, 9, 10, and 11 consider only "pointed" wings. For a rectangular wing it is necessary to treat explicitly the logical consequences of a nonpointed leading edge. The expressions for loading derived herein, therefore, differ in detail from, for example, those given in reference 10.

where $\phi$ is the perturbation velocity potential. The assumptions needed in deriving this equation are discussed in reference 11. The boundary conditions on the upper side of the xy-plane are given as follows:

For $x < 0$,

$$\phi(x,y,+0,\tau) = 0 \tag{3a}$$

for $0 \leq x \leq c$,

$$\left.\begin{aligned} \phi(x,y,+0,\tau) &= 0 && \left(|y| \geq s\right) \\ \frac{\partial \phi}{\partial z}(x,y,+0,\tau) &= y^2\left(U\frac{\partial F}{\partial x} + \frac{\partial F}{\partial \tau}\right) && \left(|y| \leq s\right) \end{aligned}\right\} \tag{3b}$$

and for $x > c$,

$$\phi(x,y,+0,\tau) = \phi(c,y,+0,\tau) \tag{3c}$$

In addition, derivatives of the potential at infinity must be zero.

The method used in reference 8 is employed herein to calculate the velocity potential $\phi(x,y,+0,\tau)$ on the top surface of the plate. Thus,

$$\phi(x,y,+0,\tau) = -\frac{1}{3}\left(U\frac{\partial F}{\partial x} + \frac{\partial F}{\partial \tau}\right)\left(\frac{s^2}{2} + y^2\right)\sqrt{s^2 - y^2} \tag{4}$$

The lift per unit area in terms of velocity potential is

$$p(x,y,\tau) = 2\rho U\left[\frac{\partial \phi(x,y,+0,\tau)}{\partial x} + \frac{1}{U}\frac{\partial \phi(x,y,+0,\tau)}{\partial \tau}\right]$$

which, upon substitution from equation (4), becomes

$$p(x,y,\tau) = -\frac{4}{3}q\left(\frac{\partial^2 F}{\partial x^2} + \frac{2}{U}\frac{\partial^2 F}{\partial x\,\partial \tau} + \frac{1}{U^2}\frac{\partial^2 F}{\partial \tau^2}\right)\left(\frac{s^2}{2} + y^2\right)\sqrt{s^2 - y^2} \tag{5}$$

As a result of applying slender-body aerodynamic theory to a rectangular plan form, the velocity potential jumps from a value of zero ahead of the leading edge to some finite value at the leading edge. Therefore, a concentrated aerodynamic load acts along the leading edge and has a magnitude given by

$$V(y,\tau) = 2\rho U\phi(0,y,+0,\tau)$$

which, upon substitution from equation (4), is given by the following equation:

$$V(y,\tau) = -\frac{4}{3}q\left[\frac{\partial F(0,\tau)}{\partial x} + \frac{1}{U}\frac{\partial F(0,\tau)}{\partial \tau}\right]\left(\frac{s^2}{2} + y^2\right)\sqrt{s^2 - y^2} \tag{6}$$

## Structural Equilibrium

The principle of minimum potential energy is used to derive the differential equation of structural equilibrium for the function $F(x,\tau)$ in a manner analogous to that used in reference 8 for the corresponding divergence problem. Accordingly, the total potential energy, consisting of the strain energy of the plate plus the potential energy of the external forces, is given by the equation

$$\Pi = \frac{D}{2}\int_0^c \int_0^s \left[w_{xx}^2 + w_{yy}^2 + 2\mu w_{xx}w_{yy} + 2(1 - \mu)w_{xy}^2\right] dx\, dy -$$

$$\int_0^c \int_0^s Pw\, dx\, dy - \int_0^s Vw(0,y,\tau)dy \tag{7}$$

where the subscripts $x$ and $y$ denote differentiation with respect to $x$ and $y$, $P$ is the total distributed loading given by

$$P = p - \rho_m t\frac{\partial^2 w}{\partial \tau^2} \tag{8}$$

and $V$ is the shear at the leading edge. (See eq. (6).) Substituting equation (1) into equation (7) and integrating yield

$$\Pi = \frac{D}{2}\int_0^c \left[\frac{s^5}{5}\left(\frac{\partial^2 F}{\partial x^2}\right)^2 + 4sF^2 + \frac{4}{3}\mu s^3 F\left(\frac{\partial^2 F}{\partial x^2}\right) + \frac{8}{3}(1-\mu)s^3\left(\frac{\partial F}{\partial x}\right)^2\right]dx - \int_0^c P_1(x,\tau)F\,dx - V_1(\tau)F(0,\tau) \tag{9}$$

where

$$P_1(x,\tau) = \int_0^s P(x,y,\tau)y^2dy \tag{10a}$$

$$V_1(\tau) = \int_0^s V(y,\tau)y^2dy \tag{10b}$$

It should be noted that the integrated loadings $P_1$ and $V_1$ are temporarily considered to be unrelated to the deflection $F$ for the purposes of performing the variation.

Use of the calculus of variations to minimize the expression for potential energy yields the differential equation

$$\frac{s^5}{5}\frac{\partial^4 F}{\partial x^4} + \frac{4}{3}(3\mu - 2)s^3\frac{\partial^2 F}{\partial x^2} + 4sF = \frac{P_1(x,\tau)}{D} \tag{11}$$

and the boundary conditions

$$\left.\begin{aligned} &\frac{s^5}{5}\frac{\partial^2 F}{\partial x^2} + \frac{2}{3}\mu s^3 F = 0 && (x = 0,c)\\ &\frac{s^5}{5}\frac{\partial^3 F}{\partial x^3} - \frac{2}{3}(4 - 5\mu)s^3\frac{\partial F}{\partial x} - \frac{V_1(\tau)}{D} = 0 && (x = 0)\\ &\frac{s^5}{5}\frac{\partial^3 F}{\partial x^3} - \frac{2}{3}(4 - 5\mu)s^3\frac{\partial F}{\partial x} = 0 && (x = c) \end{aligned}\right\} \tag{12}$$

## Aeroelastic Solution

The partial differential equation and its boundary conditions which describe the deflection of the plate due to the generalized loads $P_1(x,\tau)$ and $V_1(\tau)$ are given by equations (11) and (12). The generalized loads are expressed in terms of the deflections by substituting the expressions for aerodynamic loads (eqs. (5) and (6)) and the inertia loads (included in eq. (8)) into equations (10). Thus,

$$P_1(x,\tau) = -\frac{\pi}{12} qs^6\left(\frac{\partial^2 F}{\partial x^2} + \frac{2}{U}\frac{\partial^2 F}{\partial x\,\partial \tau} + \frac{1}{U^2}\frac{\partial^2 F}{\partial \tau^2}\right) - \rho_m t\,\frac{s^5}{5}\frac{\partial^2 F}{\partial \tau^2} \tag{13a}$$

$$V_1(\tau) = -\frac{\pi}{12} qs^6\left[\frac{\partial F(0,\tau)}{\partial x} + \frac{1}{U}\frac{\partial F(0,\tau)}{\partial \tau}\right] \tag{13b}$$

If these values of $P_1(x,\tau)$ and $V_1(\tau)$ are substituted into the differential equation (11) and into the boundary equations (12), if the resulting equations are made nondimensional by letting

$$\xi = \frac{x}{s}$$

and if the time dependence is taken to be

$$F(\xi,\tau) = f(\xi)e^{i\omega\tau}$$

the differential equation becomes

$$f^{IV}(\xi) + 4(\lambda - a_1)f''(\xi) + 4iK\sqrt{\frac{5\epsilon\lambda}{12}}\,f'(\xi) + \left[20 - K^2\left(1 + \frac{5\epsilon}{12}\right)\right]f(\xi) = 0 \tag{14}$$

and the boundary conditions are

$$\left.\begin{aligned} f''(\xi) + a_2 f(\xi) &= 0 && \left(\xi = 0, \frac{c}{s}\right) \\ f'''(\xi) + 4(\lambda - a_3) f'(\xi) + 2iK\sqrt{\frac{5\epsilon\lambda}{12}}\, f(\xi) &= 0 && (\xi = 0) \\ f'''(\xi) - 4a_3 f'(\xi) &= 0 && \left(\xi = \frac{c}{s}\right) \end{aligned}\right\} \tag{15}$$

where

$$\lambda = \frac{5\pi}{48}\frac{qs^3}{D} \tag{16a}$$

$$K = \omega\sqrt{\frac{\rho_m t s^4}{D}} \tag{16b}$$

$$\epsilon = \frac{\pi}{2}\frac{\rho s}{\rho_m t} \tag{16c}$$

and

$$a_1 = \frac{10}{3}\left(1 - \frac{3}{2}\mu\right)$$

$$a_2 = \frac{10}{3}\mu$$

$$a_3 = \frac{10}{3}\left(1 - \frac{5}{4}\mu\right)$$

It should be noted that real values of $\omega$ (or $K$) infer simple harmonic motion and should yield the flutter boundary.

The general solution of the differential equation (14) can be written

$$f(\xi) = C_1 e^{im_1\xi} + C_2 e^{im_2\xi} + C_3 e^{im_3\xi} + C_4 e^{im_4\xi} \tag{17}$$

where $m_1, m_2, m_3, m_4$, are the roots of the characteristic equation

$$m^4 - 4(\lambda - a_1)m^2 - 4K\sqrt{\frac{5\epsilon\lambda}{12}}\,m + \left[20 - K^2\left(1 + \frac{5\epsilon}{12}\right)\right] = 0 \tag{18}$$

Substitution of equation (17) into equations (15) yields

$$\left.\begin{aligned}
&\left(a_2 - m_1^2\right)C_1 + \left(a_2 - m_2^2\right)C_2 + \left(a_2 - m_3^2\right)C_3 + \left(a_2 - m_4^2\right)C_4 = 0 \\
&\left(a_2 - m_1^2\right)C_1 e^{im_1 c/s} + \left(a_2 - m_2^2\right)C_2 e^{im_2 c/s} + \left(a_2 - m_3^2\right)C_3 e^{im_3 c/s} + \\
&\quad \left(a_2 - m_4^2\right)C_4 e^{im_4 c/s} = 0 \\
&i\left[2K\sqrt{\frac{5\epsilon\lambda}{12}} + 4m_1\left(\lambda - a_3\right) - m_1^3\right]C_1 + i\left[2K\sqrt{\frac{5\epsilon\lambda}{12}} + \right. \\
&\quad \left. 4m_2\left(\lambda - a_3\right) - m_2^3\right]C_2 + i\left[2K\sqrt{\frac{5\epsilon\lambda}{12}} + 4m_3\left(\lambda - a_3\right) - m_3^3\right]C_3 + \\
&\quad i\left[2K\sqrt{\frac{5\epsilon\lambda}{12}} + 4m_4\left(\lambda - a_3\right) - m_4^3\right]C_4 = 0 \\
&-im_1\left(4a_3 + m_1^2\right)C_1 e^{im_1 c/s} - im_2\left(4a_3 + m_2^2\right)C_2 e^{im_2 c/s} - \\
&\quad im_3\left(4a_3 + m_3^2\right)C_3 e^{im_3 c/s} - im_4\left(4a_3 + m_4^2\right)C_4 e^{im_4 c/s} = 0
\end{aligned}\right\} \tag{19}$$

The condition for a nontrivial solution is obtained by setting the determinant of the coefficients equal to zero. When this determinant is expanded and simplified, the following equation is obtained:

$$(m_1 - m_2)(m_3 - m_4)\left[A_{12}(A_{34} + B_{34})e^{i(m_1+m_2)\frac{c}{s}} + A_{34}(A_{12} + B_{12})e^{i(m_3+m_4)\frac{c}{s}}\right] +$$

$$(m_1 - m_3)(m_4 - m_2)\left[A_{13}(A_{42} + B_{42})e^{i(m_1+m_3)\frac{c}{s}} + A_{24}(A_{31} + B_{31})e^{i(m_2+m_4)\frac{c}{s}}\right] +$$

$$(m_1 - m_4)(m_2 - m_3)\left[A_{14}(A_{23} + B_{23})e^{i(m_1+m_4)\frac{c}{s}} + A_{32}(A_{41} + B_{41})e^{i(m_2+m_3)\frac{c}{s}}\right] = 0 \tag{20}$$

where

$$A_{pq} = A_{qp} = -4a_2a_3 - a_2(m_p^2 + m_pm_q + m_q^2) - 4a_3m_pm_q + m_p^2m_q^2$$

$$B_{pq} = B_{qp} = 4\lambda a_2 + 2K\sqrt{\frac{5\epsilon\lambda}{12}}(m_p + m_q) + 4\lambda m_pm_q$$

Equation (20) is expressed in terms of the roots of the characteristic equation (18) which depend on the values of $\lambda$, $K$, and $\epsilon$. Expressing this dependence explicitly is impossible; therefore, the following procedure is used to find a parametric relationship: Examination of the characteristic equation shows that the roots must have the form

$$\left.\begin{aligned} m_1 &= \gamma + i\beta \\ m_2 &= \gamma - i\beta \\ m_3 &= -\gamma + i\alpha \\ m_4 &= -\gamma - i\alpha \end{aligned}\right\} \tag{21}$$

where $\gamma$ is a positive real quantity and

$$\alpha = \sqrt{\gamma^2 - 2(\lambda - a_1) + \frac{K}{\gamma}\sqrt{\frac{5\epsilon\lambda}{12}}} \tag{22a}$$

$$\beta = \sqrt{\gamma^2 - 2(\lambda - a_1) - \frac{K}{\gamma}\sqrt{\frac{5\epsilon\lambda}{12}}} \tag{22b}$$

in which

$$\frac{K}{\gamma} = \sqrt{\frac{4\left[5 - \left(\gamma^2 - \lambda + a_1\right)^2\right]}{\gamma^2\left(1 + \frac{5\epsilon}{12}\right) - \frac{5\epsilon\lambda}{12}}} \tag{23}$$

Here, only real values of $K/\gamma$ are considered and $\alpha$ and $\beta$ can be either real or pure imaginary quantities. Equations (21), (22), and (23) show that the characteristic roots can be expressed explicitly in terms of $\lambda$, $\gamma$, and $\epsilon$ and that $K$ can be found from equation (23). When $\alpha$ and $\beta$, given by equations (22), are both real, the flutter equation (20), upon substitution from equation (21), becomes

$$64\alpha\beta\left[\left(D_1 \cos\frac{2\gamma c}{s} + E_1 \cosh\frac{\alpha c}{s}\cosh\frac{\beta c}{s} + \frac{F_1}{\alpha\beta}\sinh\frac{\alpha c}{s}\sinh\frac{\beta c}{s}\right) + i\left(D_2 \sin\frac{2\gamma c}{s} + \frac{E_2}{\alpha}\sinh\frac{\alpha c}{s}\cosh\frac{\beta c}{s} + \frac{F_2}{\beta}\cosh\frac{\alpha c}{s}\sinh\frac{\beta c}{s}\right)\right] = 0 \tag{24a}$$

where

$$D_1 = -\left(2A_1A_2 + A_1B_2 + A_2B_1\right)$$

$$E_1 = \left(A_3 + \lambda B_3\right)\left[2A_3 - \left(4\gamma^2 + \alpha^2 + \beta^2\right)A_4\right] +$$

$$\left(A_4 - \lambda\right)\left[2\alpha^2\beta^2 A_4 - \left(4\gamma^2 + \alpha^2 + \beta^2\right)A_3\right]$$

$$F_1 = \left(A_3 + \lambda B_3\right)\left[2\alpha^2\beta^2 A_4 - \left(4\gamma^2 + \alpha^2 + \beta^2\right)A_3\right] +$$

$$\alpha^2\beta^2\left(A_4 - \lambda\right)\left[2A_3 - \left(4\gamma^2 + \alpha^2 + \beta^2\right)A_4\right]$$

$$D_2 = -\left(A_1B_2 - A_2B_1\right)$$

$$E_2 = \gamma\left\{\left(A_3 + \lambda B_3\right)\left[\lambda\left(8\gamma^2 + 8a_1 - 8\lambda + \frac{K^2}{\gamma^2}\frac{5\epsilon}{12}\right) - 2\left(\gamma^2 - \lambda\right)\frac{K}{\gamma}\sqrt{\frac{5\epsilon\lambda}{12}}\right] -\right.$$

$$\left.\alpha^2\left(A_4 - \lambda\right)\left[\lambda\left(8\gamma^2 + 8a_1 - 8\lambda + \frac{K^2}{\gamma^2}\frac{5\epsilon}{12}\right) + 2\left(\gamma^2 - \lambda\right)\frac{K}{\gamma}\sqrt{\frac{5\epsilon\lambda}{12}}\right]\right\}$$

$$F_2 = -\gamma\left\{\left(A_3 + \lambda B_3\right)\left[\lambda\left(8\gamma^2 + 8a_1 - 8\lambda + \frac{K^2}{\gamma^2}\frac{5\epsilon}{12}\right) + 2\left(\gamma^2 - \lambda\right)\frac{K}{\gamma}\sqrt{\frac{5\epsilon\lambda}{12}}\right] -\right.$$

$$\left.\beta^2\left(A_4 - \lambda\right)\left[\lambda\left(8\gamma^2 + 8a_1 - 8\lambda + \frac{K^2}{\gamma^2}\frac{5\epsilon}{12}\right) - 2\left(\gamma^2 - \lambda\right)\frac{K}{\gamma}\sqrt{\frac{5\epsilon\lambda}{12}}\right]\right\}$$

in which

$$A_1 = -\frac{100}{9}\left(1 - \mu\right)^2 - \frac{10}{3}\mu\gamma^2 + \left(\gamma^2 - \lambda - \frac{K}{2\gamma}\sqrt{\frac{5\epsilon\lambda}{12}}\right)^2$$

$$A_2 = -\frac{100}{9}(1-\mu)^2 - \frac{10}{3}\mu\gamma^2 + \left(\gamma^2 - \lambda + \frac{K}{2\gamma}\sqrt{\frac{5\epsilon\lambda}{12}}\right)^2$$

$$B_1 = \frac{20}{3}(1-\mu)\lambda + \left(\gamma^2 - \lambda\right)\left(2\lambda + \frac{K}{\gamma}\sqrt{\frac{5\epsilon\lambda}{12}}\right)$$

$$B_2 = \frac{20}{3}(1-\mu)\lambda + \left(\gamma^2 - \lambda\right)\left(2\lambda - \frac{K}{\gamma}\sqrt{\frac{5\epsilon\lambda}{12}}\right)$$

$$A_3 = \frac{100}{9}(1-\mu)(1-2\mu) - \frac{20}{3}(1-\mu)\lambda + \frac{10}{3}(1-\mu)\gamma^2 + \lambda^2 - \frac{K^2}{4\gamma^2}\frac{5\epsilon\lambda}{12}$$

$$A_4 = \frac{10}{3}(1-\mu) + \gamma^2$$

$$B_3 = \frac{10}{3}\mu - \gamma^2$$

and the expressions for $\alpha$, $\beta$, and $K/\gamma$ are given by equations (22) and (23). If $\alpha$ is real and $\beta$ is imaginary in equations (22), the flutter equation (20) has the form

$$i64\alpha\beta_1\left[\left(D_1 \cos\frac{2\gamma c}{s} + E_1 \cosh\frac{\alpha c}{s}\cos\frac{\beta_1 c}{s} + \frac{F_1}{\alpha\beta_1}\sinh\frac{\alpha c}{s}\sin\frac{\beta_1 c}{s}\right) + i\left(D_2 \sin\frac{2\gamma c}{s} + \frac{E_2}{\alpha}\sinh\frac{\alpha c}{s}\cos\frac{\beta_1 c}{s} + \frac{F_2}{\beta_1}\cosh\frac{\alpha c}{s}\sin\frac{\beta_1 c}{s}\right)\right] = 0 \qquad (24b)$$

where

$$\beta_1 = \sqrt{-\gamma^2 + 2\left(\lambda - a_1\right) + \frac{K}{\gamma}\sqrt{\frac{5\epsilon\lambda}{12}}}$$

If both $\alpha$ and $\beta$ are imaginary, equation (20) becomes

$$-64\alpha_1\beta_1\left[\left(D_1 \cos\frac{2\gamma c}{s} + E_1 \cos\frac{\alpha_1 c}{s}\cos\frac{\beta_1 c}{s} + \frac{F_1}{\alpha_1\beta_1}\sin\frac{\alpha_1 c}{s}\sin\frac{\beta_1 c}{s}\right) + i\left(D_2 \sin\frac{2\gamma c}{s} + \frac{E_2}{\alpha_1}\sin\frac{\alpha_1 c}{s}\cos\frac{\beta_1 c}{s} + \frac{F_2}{\beta_1}\cos\frac{\alpha_1 c}{s}\sin\frac{\beta_1 c}{s}\right)\right] = 0 \qquad (24c)$$

where

$$\alpha_1 = \sqrt{-\gamma^2 + 2(\lambda - a_1) - \frac{K}{\gamma}\sqrt{\frac{5\epsilon\lambda}{12}}}$$

Equation (24a), (24b), or (24c) can be solved by the following trial-and-error process: First, values of $\lambda$ and $\epsilon$ are assigned; then, for varying values of $\gamma$, both the real and imaginary parts of the proper form of equations (24) are solved for the corresponding values of $c/s$ where they exist. Only for particular values of $\gamma$ will these two solutions yield identical values of $c/s$. By finding these particular values of $\gamma$, the appropriate values of $c/s$ associated with the assigned values of $\lambda$ and $\epsilon$ are determined. Some results obtained by this and subsequent procedures are presented and discussed in a later section.

## Solution for Large Values of $c/s$

The results in the region where $c/s$ is large show that $\alpha$ is real and $\beta$ is imaginary. In this region, equation (24b), upon consideration of the order of magnitude of its terms, reduces to

$$E_1 \cos\frac{\beta_1 c}{s} + \frac{F_1}{\alpha\beta_1}\sin\frac{\beta_1 c}{s} + i\left(\frac{E_2}{\alpha}\cos\frac{\beta_1 c}{s} + \frac{F_2}{\beta_1}\sin\frac{\beta_1 c}{s}\right) = 0 \qquad (25)$$

This equation can be satisfied only when

$$E_1F_2 - \frac{E_2F_1}{\alpha^2} = 0$$

which, when expanded, becomes

$$\frac{2\gamma}{\alpha^2}\left[8\gamma^2\left(\gamma^2 + a_1 - \lambda\right) + \frac{K^2}{\gamma^2}\frac{5\epsilon\lambda}{12}\right]\left[\left(A_3 + \lambda B_3\right)^2 + \alpha^2\beta_1{}^2\left(A_4 - \lambda\right)^2\right]\left[\left(2\lambda - \right.\right.$$

$$\left.\left.\frac{K}{\gamma}\sqrt{\frac{5\epsilon\lambda}{12}}\right)A_3 + \left(2\lambda + \frac{K}{\gamma}\sqrt{\frac{5\epsilon\lambda}{12}}\right)\alpha^2 A_4\right] = 0$$

Only the last factor of this equation yields a solution:

$$\left(2\lambda - \frac{K}{\gamma}\sqrt{\frac{5\epsilon\lambda}{12}}\right)A_3 + \left(2\lambda + \frac{K}{\gamma}\sqrt{\frac{5\epsilon\lambda}{12}}\right)\alpha^2 A_4 = 0 \tag{26}$$

The value of $c/s$ corresponding to the solution of equation (26) can be found from equation (25) to be

$$\frac{c}{s} = \frac{1}{\beta_1}\tan^{-1}\frac{-\alpha\beta_1 E_1}{F_1} \tag{27}$$

Equations (26) and (27) are used to find the variation of $\lambda$ with $c/s$ for various values of $\epsilon$ in the region where $c/s$ is large. That is, values of $\lambda$ and $\epsilon$ are assigned and $\gamma$ is varied until the two values of $\gamma$ (there are either two or none of them) are found that satisfy equation (26). Then, the corresponding values of $c/s$ are given by equation (27).

## Mode Shapes

The components of normalized mode shape $\frac{f(\xi)}{f(0)}e^{i\omega\tau}$ which are in phase and out of phase with the maximum leading-edge deflection are given by $\left[\frac{f(\xi)}{f(0)}\right]_R$ and $\left[\frac{f(\xi)}{f(0)}\right]_I$, which are the real and imaginary parts, respectively, of the function

$$\frac{f(\xi)}{f(0)} = \frac{C_1 e^{im_1\xi} + C_2 e^{im_2\xi} + C_3 e^{im_3\xi} + C_4 e^{im_4\xi}}{C_1 + C_2 + C_3 + C_4} \tag{28}$$

Here, the constants $C_2$, $C_3$, and $C_4$ are found from the boundary equations (19) in terms of $C_1$ to be, respectively,

$$C_2 = \frac{C_1}{\Delta}\left[\left(m_3 - m_4\right)\left(a_2 - m_1^2\right)A_{34}e^{-i\left(m_1+m_2\right)\frac{c}{s}} + \left(m_4 - m_1\right)\left(a_2 - m_3^2\right)A_{14}e^{-i\left(m_2+m_3\right)\frac{c}{s}} + \left(m_1 - m_3\right)\left(a_2 - m_4^2\right)A_{13}e^{-i\left(m_2+m_4\right)\frac{c}{s}}\right]$$

$$C_3 = \frac{C_1}{\Delta}\left[\left(m_4 - m_2\right)\left(a_2 - m_1^2\right)A_{24}e^{-i\left(m_1+m_3\right)\frac{c}{s}} + \left(m_1 - m_4\right)\left(a_2 - m_2^2\right)A_{14}e^{-i\left(m_2+m_3\right)\frac{c}{s}} + \left(m_2 - m_1\right)\left(a_2 - m_4^2\right)A_{12}e^{-i\left(m_3+m_4\right)\frac{c}{s}}\right]$$

$$C_4 = \frac{C_1}{\Delta}\left[\left(m_2 - m_3\right)\left(a_2 - m_1^2\right)A_{23}e^{-i\left(m_1+m_4\right)\frac{c}{s}} + \left(m_3 - m_1\right)\left(a_2 - m_2^2\right)A_{13}e^{-i\left(m_2+m_4\right)\frac{c}{s}} + \left(m_1 - m_2\right)\left(a_2 - m_3^2\right)A_{12}e^{-i\left(m_3+m_4\right)\frac{c}{s}}\right]$$

where

$$\Delta = \left(m_2 - m_4\right)\left(a_2 - m_3^2\right)A_{24}e^{-i\left(m_1+m_3\right)\frac{c}{s}} + \left(m_3 - m_2\right)\left(a_2 - m_4^2\right)A_{23}e^{-i\left(m_1+m_4\right)\frac{c}{s}} + \left(m_4 - m_3\right)\left(a_2 - m_2^2\right)A_{34}e^{-i\left(m_1+m_2\right)\frac{c}{s}}$$

## Approximate Solutions

In practical wing construction, an exact solution, such as that obtained in the previous sections, would not be feasible and some sort of approximation of the chordwise deflection shape would be necessary. One method of approximation is to represent the chordwise variation of deflection by the first few terms of a power series. The present configuration (fig. 1) is used to test the accuracy of such an approximation.

In this approximate analysis, the assumed chordwise deflection shape

$$F(x,\tau) = \left[d_0 + d_1\left(\frac{x}{s}\right) + d_2\left(\frac{x}{s}\right)^2 + d_3\left(\frac{x}{s}\right)^3 + \ldots\right]e^{i\omega\tau} \tag{29}$$

is substituted into equation (9), the equation for potential energy. Minimization of the potential energy with respect to $d_0$, $d_1$, $d_2$, $d_3$ . . . and then substitution of the appropriate expressions for $P_1(x,\tau)$ and $V_1(\tau)$ from equations (13) yield a set of homogeneous simultaneous equations. The solution of these equations is obtained by setting the determinant of the coefficients equal to zero. Cubic approximation of the chordwise variation of deflection results in the following complex equation:

$$\begin{vmatrix}
b + 12K\sqrt{\frac{5\epsilon\lambda}{12}} & \frac{1}{2}b + 4\lambda\frac{s}{c} + 14K\sqrt{\frac{5\epsilon\lambda}{12}} & \frac{1}{3}b + \left(8\lambda + \frac{20}{3}\mu\right)\frac{s}{c} + 14K\sqrt{\frac{5\epsilon\lambda}{12}} & \frac{1}{4}b + (12\lambda + 10\mu)\frac{s}{c} + 14K\sqrt{\frac{5\epsilon\lambda}{12}} \\
\frac{1}{2}b & \frac{1}{3}b + \frac{40}{3}(1-\mu)\frac{s}{c} + 12K\sqrt{\frac{5\epsilon\lambda}{12}} & \frac{1}{4}b + \left[4\lambda + \frac{40}{3}(4-3\mu)\right]\frac{s}{c} + 1\frac{8}{3}K\sqrt{\frac{5\epsilon\lambda}{12}} & \frac{1}{5}b + \left[8\lambda + \frac{20}{3}(2-\mu)\right]\frac{s}{c} + 13K\sqrt{\frac{5\epsilon\lambda}{12}} \\
\frac{1}{3}b + \frac{20}{3}\mu\frac{s}{c} & \frac{1}{4}b + \frac{40}{3}(4-3\mu)\frac{s}{c} + 1\frac{4}{3}K\sqrt{\frac{5\epsilon\lambda}{12}} & \frac{1}{5}b + \left[\frac{8}{3}\lambda + \frac{40}{9}(4-3\mu)\right]\frac{s}{c} + 4\frac{s^3}{c^3} + 12K\sqrt{\frac{5\epsilon\lambda}{12}} & \frac{1}{6}b + \left[6\lambda + \frac{20}{3}(3-2\mu)\right]\frac{s}{c} + 6\frac{s^3}{c^3} + 1\frac{12}{5}K\sqrt{\frac{5\epsilon\lambda}{12}} \\
\frac{1}{4}b + 10\mu\frac{s}{c} & \frac{1}{5}b + \frac{20}{3}(2-\mu)\frac{s}{c} + 11K\sqrt{\frac{5\epsilon\lambda}{12}} & \frac{1}{6}b + \left[2\lambda + \frac{20}{9}(3-2\mu)\right]\frac{s}{c} + 6\frac{s^3}{c^3} + 1\frac{8}{3}K\sqrt{\frac{5\epsilon\lambda}{12}} & \frac{1}{7}b + \left[\frac{24}{5}\lambda + 8(3-2\mu)\right]\frac{s}{c} + 12\frac{s^3}{c^3} + 12K\sqrt{\frac{5\epsilon\lambda}{12}}
\end{vmatrix} = 0 \tag{30}$$

where

$$b = \left[20 - K^2\left(1 + \frac{5\epsilon}{12}\right)\right]\frac{c}{s}$$

By a trial-and-error solution, the flutter-frequency parameter K is eliminated and the variation of $\lambda$ with $c/s$ is found for a given value of $\epsilon$. The equation for parabolic deformation, obtained from equation (30) by deleting the last row and last column, is solved analytically for $\lambda$ in terms of $c/s$ and $\epsilon$.

## RESULTS AND DISCUSSION

Results of the flutter analysis, in which chordwise variation of deflection is allowed complete freedom, are given by the flutter boundaries in figure 2. For convenience, these boundaries are denoted herein as "exact." The variation of dynamic-pressure parameter $\lambda$ with $c/s$ is given for two values of mass-ratio parameter $\epsilon$. Here, and in the other results presented in this section, Poisson's ratio is taken equal to 1/3. Comparison with the static aeroelastic-divergence boundary, obtained from reference 8, shows that divergence is less critical than flutter.

Each flutter boundary, for large values of $c/s$, consists of a series of scallops approaching a limiting value of $\lambda$. The variation of this limiting value of $\lambda$ with $\epsilon$ is given in figure 3. The flutter speed is less than the divergence speed and seems to approach it asymptotically for high values of $\epsilon$.

Mode shapes, showing the chordwise variation of deflection at flutter, are obtained from the analysis and are shown in figure 4 for two values of $c/s$ which correspond to the positions indicated by the tick marks on the curve for $\epsilon = 0.01$ in figure 2. Increasing $c/s$ (decreasing the aspect ratio) adds more waves to the mode shape.

Flutter boundaries, obtained from parabolic and cubic approximations of the chordwise deflection shape, are compared with the exact flutter boundary in figure 5. Both approximations yield good results for values of $c/s$ less than 3, with the cubic curve yielding almost exact results. However, for higher values of $c/s$ both approximations yield poor results. Apparently, in order to analyze the flutter behavior of wings in this region, higher order terms in the chordwise deflection shape must be used.

## CONCLUDING REMARKS

The present flutter analysis of rectangular plates of very low aspect ratio indicates that the flutter-mode shape has an increasing number of waves in the chordwise direction as the aspect ratio is decreased. Approximation of the chordwise deflection shape by use of parabolic or cubic curves yields flutter speeds in fair agreement with those of the "exact" theory

for a ratio of chord to semispan less than 3 with the cubic approximation giving almost exact results. For lower aspect ratios, higher order approximations must be used.

Langley Aeronautical Laboratory,
National Advisory Committee for Aeronautics,
Langley Field, Va., February 17, 1958.

## REFERENCES


1. Miles, John W.: On the Improbability of Low Aspect Ratio Wing Flutter. Rep. AL-1236, North American Aviation, Inc., Jan. 30, 1951.

2. Voss, Herbert M., and Hassig, Hermann J.: Introductory Study of Flutter of Low-Aspect-Ratio Wings at Subsonic Speeds. Contract No. NOa(s) 51-109-c, M.I.T., Dept. Aero. Eng., May 1, 1952.

3. Voss, Herbert M., Zartarian, Garabed, and Hsu, Pao-Tan: Application of Numerical Integration Techniques to the Low-Aspect-Ratio Flutter Problem in Subsonic and Supersonic Flows. ASRL Tech. Rep. No. 52-3 (Contract No. NOa(s) 53-564-c), M.I.T., Dept. Aero. Eng., Oct. 1, 1954.

4. Liban, E., Neuringer, J., and Rabinowitz, S.: The Flutter Analysis of an Elastic Wing With Supersonic Edges. Rep. No. E-SAF-1, Republic Aviation Corp., Mar. 23, 1953.

5. Voss, Herbert M., Zartarian, Garabed, and Hsu, Pao-Tan: Theoretical and Experimental Investigation of the Aeroelastic Behavior of Low-Aspect-Ratio Wings. Contract No. NOa(s) 51-109-c, M.I.T., Dept. Aero. Eng., June 15, 1953.

6. Hsu, Pao-Tan, Martuccelli, John R., and Ashley, Holt: Oscillatory Aerodynamic Loads on Low-Aspect-Ratio Wings in Subsonic Flow. Part I. Methods of Calculation and Comparison With Measured Loads. ASRL Tech. Rep. 52-4 (Contract No. NOa(s) 53-564-c), M.I.T., Dept. Aero. Eng., Dec. 1, 1955.

7. Leyds, J.: Aeroelastic Problems of Low Aspect Ratio Wings. Part IV. Application of the Structural and Aerodynamic Matrices to the Solution of the Flutter Problem. Aircraft Engineering, vol. XXVIII, no. 327, May 1956, pp. 166-167.

8. Hedgepeth, John M., and Waner, Paul G., Jr.: Analysis of Static Aeroelastic Behavior of Low-Aspect-Ratio Rectangular Wings. NACA TN 3958, 1957.

9. Jones, Robert T.: Properties of Low-Aspect-Ratio Pointed Wings at Speeds Below and Above the Speed of Sound. NACA Rep. 835, 1946. (Supersedes NACA TN 1032.)

10. Garrick, I. E.: Some Research on High-Speed Flutter. Third Anglo-American Aero. Conf., Sept. 4-7, 1951 (Brighton, England). R.A.S., 1952, pp. 419-446J.

11. Miles, John W.: On Non-Steady Motion of Slender Bodies. Aero. Quarterly, vol. II, pt. III, Nov. 1950, pp. 183-194.

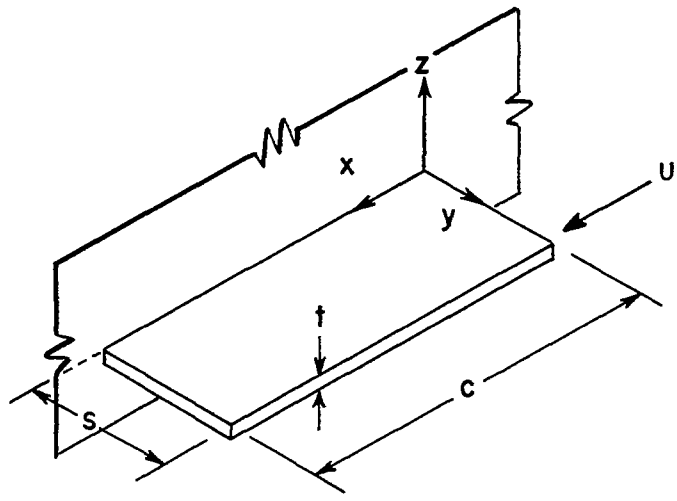


Figure 1.- Cantilever plate of very low aspect ratio.

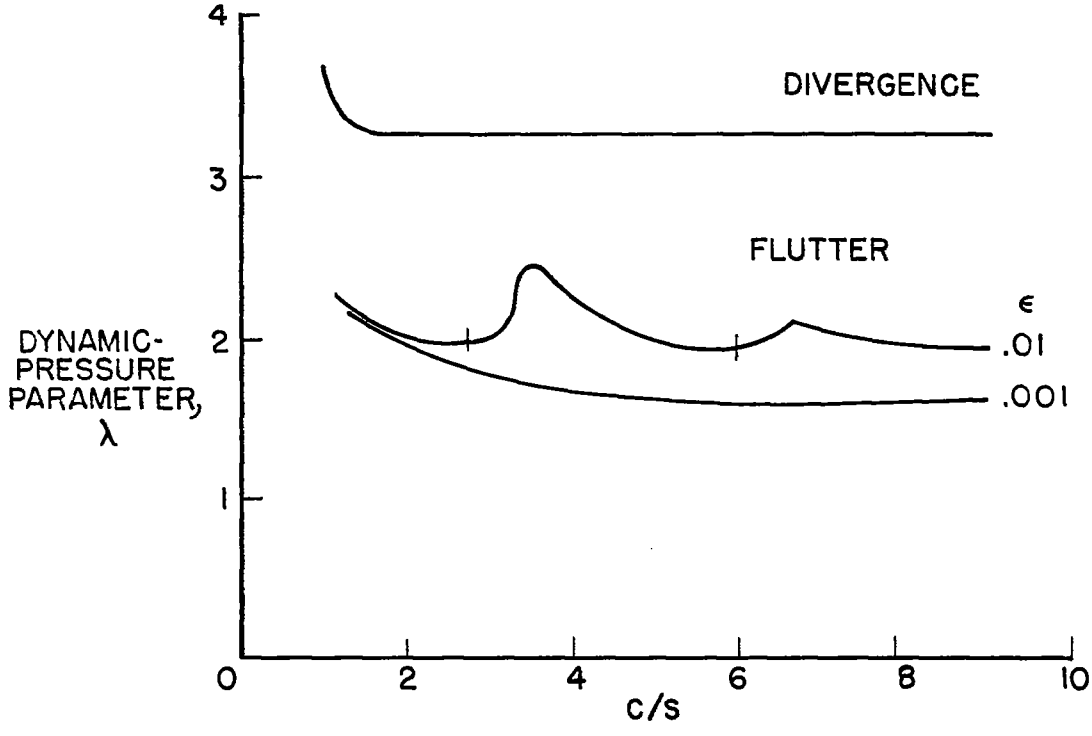


Figure 2.- Flutter boundaries obtained by exact analysis. $\mu = \frac{1}{3}$; $\lambda = \frac{10\pi}{9} \frac{q}{E}\left(\frac{s}{t}\right)^3$; $\epsilon = \frac{\pi}{2} \frac{\rho s}{\rho_m t}$.

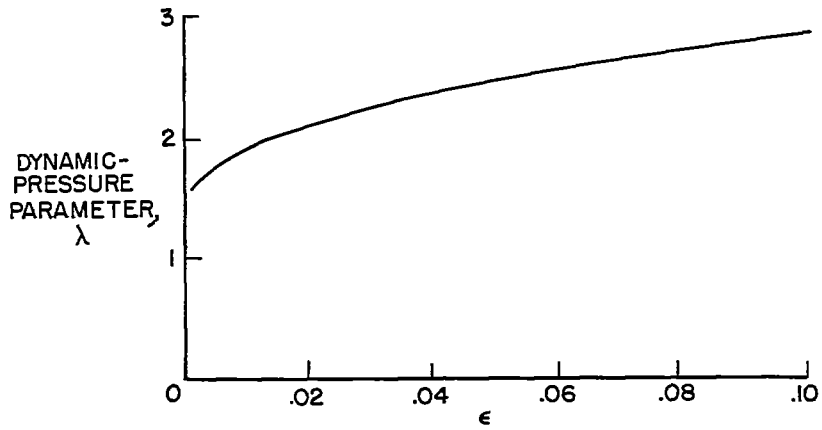


Figure 3.- Limiting value of critical dynamic-pressure parameter for flutter. $\mu = \frac{1}{3}$.

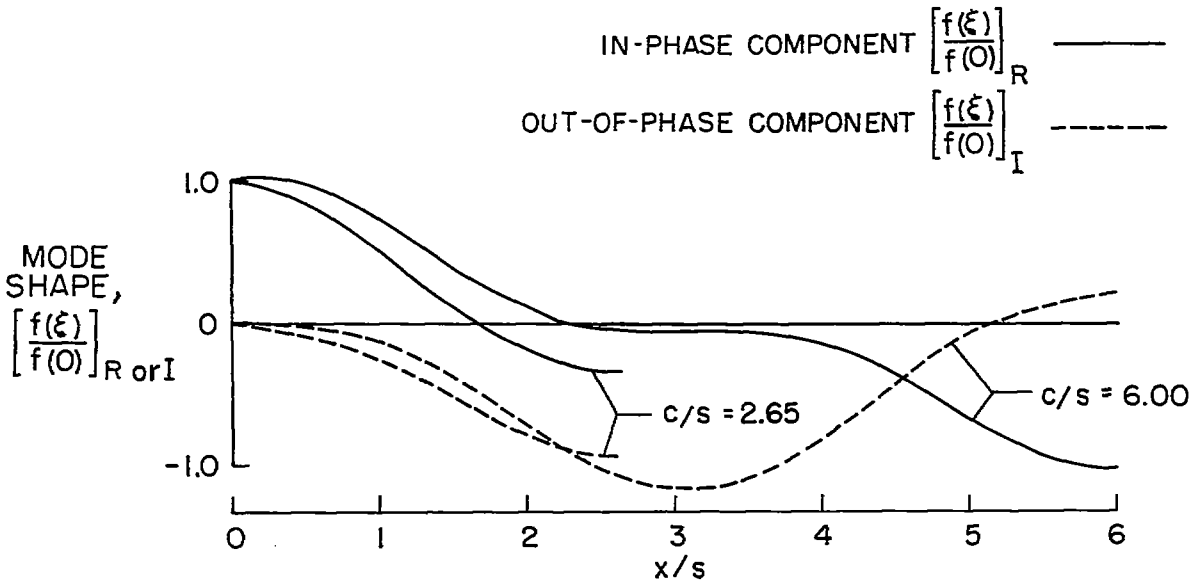


Figure 4.- Chordwise variation of deflection at flutter. $\mu = \frac{1}{3}$; $\epsilon = 0.01$.

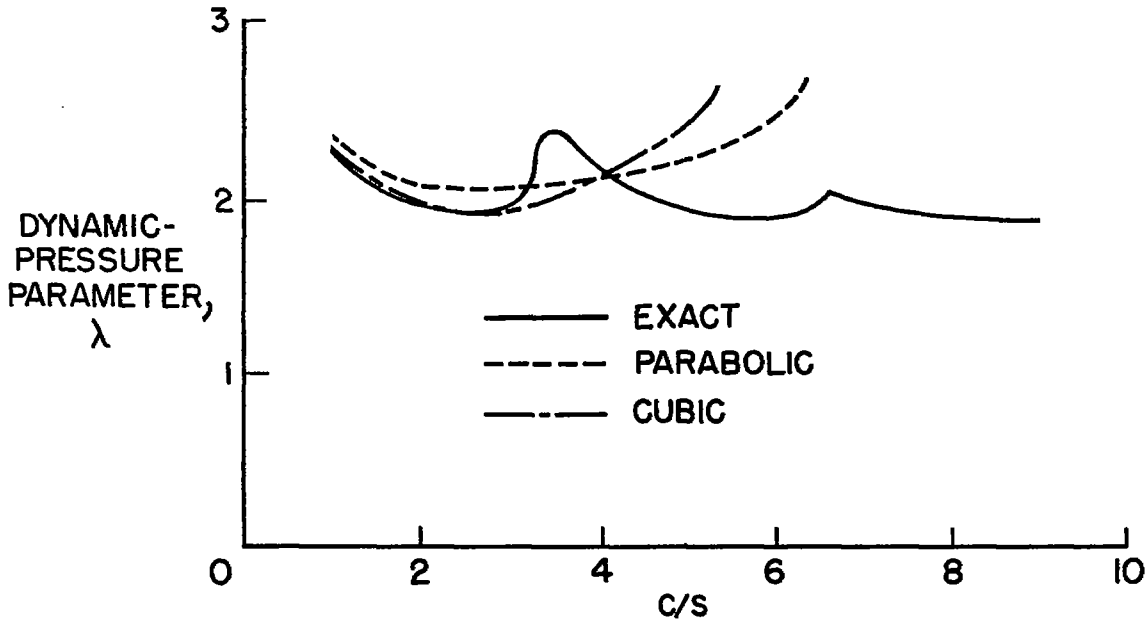


Figure 5.- Comparison of exact and approximate flutter boundaries. $\mu = \frac{1}{3}$; $\epsilon = 0.01$.